Pergamon

Cement and Concrete Research 31 (2001) 1467–1477

CEMENT AND CONCRETE RESEARCH

Effect of drying on cement-based materials pore structure as identified by mercury intrusion porosimetry
A comparative study between oven-, vacuum-, and freeze-drying

C. Gallé*

Direction de l'Energie Nucléaire DPC/SCCME/LECBA, CEA-Centre de Saclay, Bat. 158, 91191 Gif-sur-Yvette Cedex, France

Received 14 November 2000; accepted 25 June 2001

Abstract

Diffusive and convective transport properties are essential for cement-based materials durability studies. To understand and model such transport mechanisms, information on physical intrinsic parameters such as porosity and pore structure is needed. Mercury intrusion porosimetry (MIP) has been used for a long time as a convenient means for porous space investigation. This method requires complete material water removal, generally achieved through various drying procedures. In this context, the effects of four drying methods (oven-drying at 60°C and 105°C, vacuum-drying, and freeze-drying—sublimation) on porosity and pore structure determined by MIP, were compared. Experimental measurements were performed on CEM I (OPC) and CEM V (blastfurnace slag–pulverised fuel ash, BFS–PFA) pure cement pastes and concretes. Results confirmed that oven-drying generates important damages for the materials microstructure in the capillary porosity domain and confirmed the applicability of the freeze-drying technique as a suitable drying procedure to investigate cement-based materials pore structure using MIP. © 2001 Elsevier Science Ltd. All rights reserved.

Keywords: Radioactive waste; Cement paste; Concrete; Drying; Microstructure

1. Introduction

Cement-based materials (grout, concrete) have long been used in nuclear industry particularly for low-level waste (LLW) and intermediate-level waste (ILW) management. Their good compatibility with various kinds of solid and liquid wastes, their long-term durability, and radionuclides retention capacity make these materials essential for waste conditioning, for containers, and for the elaboration of disposal engineered barriers [1,2]. Moreover, concrete materials could widely be used as structural elements for surface long-term interim storage. For many years, CEA (French Atomic Energy Commission) has been involved in numerous research programmes related to the long-term behaviour of cement-based materials for nuclear wastes. Studies were carried out in various fields such as: cement pastes and concretes chemical degradation [3–6] and associated mechanical properties [7], α, β, and γ radiolysis of alkaline interstitial solution [8], effect of carbonates [9] and sulfates [10,11], diffusive properties [12] and gas transport ability [13], and radionuclides migration. Durability of cement-based materials—resistance capacity to aggressive environments—strongly depends on their transport properties. The more permeable the materials, the more the aggressive species have the possibility to penetrate and generate potential damages. Therefore, transport properties have to be studied in strong relationship with material microstructural features (porosity, pore size).

Porous space characterisation can be reached by different methods: gas adsorption, vapor sorption, thermoporometry, mercury porosimetry, and image analysis. The main objective is to obtain reproducible and meaningful microstructural parameters to correlate them to physical properties. Mercury intrusion porosimetry (MIP) has been successfully used for a long time [14–27]. An MIP test demands complete water removal from the specimen (a few cubic centimeters). Several techniques can be applied to reach full desaturation: oven-drying at temperatures usually between 50°C and 105°C, vacuum-drying, freeze-drying (sublimation), solvent replacement drying, and D-drying [21,28,29].

* Tel.: +33-1-69-08-86-39; fax: +33-1-69-08-84-41.
E-mail address: galle@cea.fr (C. Gallé).

0008-8846/01/$ – see front matter © 2001 Elsevier Science Ltd. All rights reserved.
PII: S0008-8846(01)00594-4

These techniques are often used without clearly knowing the way they can affect the microstructural information itself. As is well known, hardened cement-based materials are very sensitive to hydric conditions. Desaturation, desorption, and dehydration phenomena associated to drying may generate damages like microcracking, capillary porosity evolution, fine pores collapse, mineralogical transformations. Thus, the removal of evaporable pore water may introduce significant degradation of the pore structure. To ignore such potential effects may lead to the alteration of porous space characteristics.

The purpose of this study was to compare the effects of several drying techniques on total free water porosity and pore structure identified by MIP of hardened cement pastes and concretes. Materials were prepared with two French industrial cements. Two temperatures were considered for the oven-drying tests: 60°C and 105°C. Vacuum-drying (10^{-1} Pa) tests were carried out at ambient temperature and freeze-drying operations (sublimation) were performed with a standard freeze-dryers. In order to make sure of the representativeness of porous space intrinsic characteristics and to limit microstrutural damaging, the best pretreatment was suggested.

2. Materials

The experimental programme was carried out with pure hardened cement pastes. All the materials were prepared with French industrial CEM I and CEM V cement types (Table 1). The CEM I cement is a standard OPC cement from Lafarge Cements (Teil factory) and the CEM V cement is a BFS–PFA cement (blastfurnace slag–pulverised fuel ash) from Origny Cements (Lumbres factory). Cement pastes can be regarded as homogeneous materials well adapted to investigate basic mechanisms. In spite of the potential effect of aggregates, complementary work with two concretes based on the same cements was also undertaken. Pure cement pastes were prepared with various water-cement (w/c) ratios 0.30, 0.40, and 0.50. Concrete mix designs are given in Table 2. Pure pastes were cured under $Ca(OH)_2$ water saturated for 4 months at 20°C. CEM I and CEM V concretes were cured in sealed bags for around 5 and 12 months, respectively.

Table 1
Average characteristics of CEM I (OPC) and CEM V (BFS–PFA) cements

Components (%)	CEM I cement	CEM V cement
Clinker	100	51
Slag	–	25
Fly ash	–	24
Gypsum added (%)	7	4
Chemical composition (>0.2%)		
SiO_2	23.7	29.0
Al_2O_3	2.8	10.8
Fe_2O_3	2.3	3.3
CaO	67.3	45.5
MgO	0.7	2.5
SO_3	1.9	2.6
K_2O/Na_2O	0.2	1.5
Density (g/cm^3)	3.20	2.90
Specific area (cm^2/g)	3105	4700
Shrinkage, 28 days (μm)	554	720
Compressive strength, 28 days (MPa)	60	46

Table 2
CEM I (OPC) and CEM V (BFS–PFA) concretes mix designs (kg/m^3)

Components	Quantity
CEM I concrete	
Silica–calcareous aggregate 8/20 mm	800
Silica–calcareous aggregate 4/12 mm	400
Silica–calcareous sand 0/4 mm	750
Cement CEM I	350
Water	150
Plasticizer	1.8
Water cement ratio (w/c)	0.43
CEM V concrete	
Silica–calcareous aggregate 10/14 mm	600
Silica–calcareous aggregate 4/10 mm	520
Silica–calcareous sand 0/4 mm	665
Cement CEM V	400
Water	166
Plasticizer	6.0
Water cement ratio (w/c)	0.43

3. Experimental porosity measurement and microstructural investigation

The materials porous space was characterised through total free water porosity measurements and MIP tests. As is well known, the MIP technique does not give representative values of total porosity. This method is generally limited to pore accesses from around 375 to 0.003 μm. Total mercury porosities for cement pastes will be thus provided only for information.

Total water porosity (ϕ_w) was estimated by measuring the total water amount removed from water saturated samples after each drying procedure until stable mass loss. Total porosity was calculated as follows (Eq. (1)):

$$\phi_w = \frac{m_s - m_d}{v\rho} \quad (1)$$

where ϕ_w is the total water porosity, m_s is the sample water saturated mass (kg), m_d is the sample dried mass (kg), v is the sample volume (m^3), and ρ is the water density at 20°C (kg/m^3).

MIP is a method that consists of isostatically injecting, under very high pressure (several hundred megapascals), a nonwetting fluid (mercury) into the porous material. The test is governed by the Washburn–Laplace equation in which the size of intruded pore accesses, assimilated to

cylindrical capillaries, are inversely proportional to the applied pressure (Eq. (2)):

$$P = \frac{4\gamma\cos\theta}{d} \quad (2)$$

where P is the mercury injection pressure (Pa), γ is the surface tension of mercury (N/m), θ is the contact angle between solid and mercury (°), and d is the pore access diameter (m).

MIP tests were performed with a Micromeritics Autopore II 9220 mercury porosimeter with a maximum 413 MPa injection pressure. By assuming a contact angle of 130° and a mercury surface tension of 484×10^{-3} N/m, the minimum pore access diameter reached is about 3×10^{-9} m. The mercury porosity (ϕ_{Hg}) is defined as the ratio between the total injected mercury volume and the total volume of the sample.

4. Experimental drying procedures

Four drying methods were used for this study: oven-drying at 60°C and 105°C, vacuum-drying, and freeze-drying. Many laboratories use these techniques applying specific procedures. Oven-drying at 105°C is probably the most widely used technique [19,20,22,25]. General methodology for each method is described hereafter.

After curing, cement paste probes (∅ 40 mm, H 80 mm) were sliced into 5-mm thick disks. The disks were sampled in the middle part of the probes to limit data dispersion. Then, specimens were dried through the different methods mentioned above until constant mass loss was reached. After drying, water porosities obtained from each method were determined by mass loss difference. The central part of the disks was then sampled for mercury intrusion tests. For the concretes, drying tests were performed on bigger probes (∅ 40 mm, H 80 mm and ∅ 113 mm, H 220 mm). Water porosity measurements were carried out with 80-mm high probes with a diameter of 40 mm. For MIP tests, the specimens were sampled in the probe's centre. The data obtained with each method were then analysed and compared.

For oven-drying tests, paste samples were placed in ventilated ovens, regulated at 60°C and 105 ± 1°C. Drying operations (approximately 7 days in duration) were achieved in extremely well-controlled conditions. No heating rates were used for these drying procedures (direct drying) except for CEM I concrete (1°C/min). After drying, samples were stored in sealed containers with silica gel to prevent rehydration.

For vacuum-drying tests, similar paste samples—as indicated above—were introduced in a vacuum device consisting in a vacuum chamber—a glass desiccator—and a vacuum pump allowing to apply a vacuum about 10^{-1} Pa. Extracted water was continuously collected in a nitrogen trap. In its principle, this method is very similar to the D-drying method for which a vacuum desiccator connected to a trap held at the temperature of a dry ice–alcohol bath is used [29].

The freeze-drying technique is commonly used in many industrial areas like soil engineering, food industry, and biology [30]. It was applied to cement-based materials in framework of this study. Concerning the experimental procedure, samples were first frozen (− 195°C) by immersion in liquid nitrogen during 5 min. This quick quenching process at very low temperature allows to generate ice microcrystals. This process prevents the growth of big ice crystals that form in larger pores and generate compressive stress in finer porosity zones that are not totally frozen. In such conditions, water drainage and finer pore retraction can be observed. Moreover, the smaller the pore access, the lower the water freezing temperature [23]. It was also demonstrated that ice formation in hardened cement paste greatly depends on sample entire moisture history and thus on w/c ratio [31]. After freezing, samples (hardened cement pastes) were introduced in an Alpha I/5 Martin Christ type freeze-dryer in which temperature and vacuum were kept to − 40°C and to 10^{-1} Pa, respectively. Concrete samples were freeze-dried using a Virtis Genesis 12ES apparatus (temperature, − 20°C, vacuum, 6 Pa). This operation allows to sublimate the ice trapped in the material porosity. It should be noticed that previous studies performed on hardened cement pastes and mortars identified the freeze-drying technique as a suitable procedure as far as MIP investigation is concerned [28,32].

Before going further on, it is important to mention here another quite popular drying technique based on the replacement of pore water by an organic solvent (solvent exchange method). This technique was initially developed by Parrott [33–35] for pore structure investigation and transport properties determination of hydrated systems [36]. Since these previous works, numerous studies on solvent replacement have been undertaken and arguments have been provided to consider that this drying technique was less damaging for the original microstructure of hydrated cement-based materials [21,28,37–39]. However, different works suggested that some solvents may react with cement hydration products during the exchange process and thus may alter their microstructure [36,40–42]. Discussions and investigations are still under way in this field [43,44]. The solvent replacement technique was not used in the framework of this study.

5. Results and discussion

5.1. Total porosity

Total water porosity values according to drying techniques for CEM I and CEM V pure cement pastes are given in Table 3. Mercury porosity values are provided for information only. The threshold pore access diameter was also

Table 3
Water porosity (ϕ_w), mercury porosity (ϕ_{Hg}), and threshold pore access diameter values for CEM I and CEM V pure cement hardened pastes

Drying method	w/c of the sample reference, CEM I paste	ϕ_w (%)	ϕ_{Hg} (%)	Threshold pore access diameter (μm)	w/c of the sample reference, CEM V paste	ϕ_w (%)	ϕ_{Hg} (%)	Threshold pore access diameter (μm)
Oven-drying 105°C	0.30	31.5	16.6	0.14	0.30	35.0	22.3	0.09
Oven-drying 60°C	0.30	26.6	17.3	0.12	0.30	29.2	22.2	0.07
Vacuum-drying	0.30	25.8	14.5	0.09	0.30	28.1	21.7	0.06
Freeze-drying	0.30	24.1	14.6	0.07	0.30	21.5	22.9	0.04
Oven-drying 105°C	0.40	37.5	22.6	0.17	0.40	42.3	29.4	0.12
Oven-drying 60°C	0.40	33.9	23.4	0.10	0.40	38.1	30.8	0.09
Vacuum-drying	0.40	33.6	23.9	0.06	0.40	36.4	32.2	0.06
Freeze-drying	0.40	30.6	22.1	0.03	0.40	33.5	32.5	0.04
Oven-drying 105°C	0.50	43.3	29.5	0.18	0.50	47.9	36.2	0.12
Oven-drying 60°C	0.50	37.3	27.8	0.12	0.50	43.4	38.6	0.09
Vacuum-drying	0.50	37.7	27.4	0.07	0.50	44.9	38.3	0.06
Freeze-drying	0.50	35.0	29.6	0.05	0.50	42.6	39.3	0.05

determined. For the concretes, water porosity was estimated only after oven-drying. For the CEM I concrete, estimated porosities were 9.7% and 10.0% at 60°C and 105°C, respectively. Water porosity values for the CEM V concrete were, respectively, about 10.1% and 10.7% at 60°C and 105°C. An average porosity of about 10% can therefore be considered for those materials. Average relative error on experimental water porosity is about 1%.

The water porosity data obtained for cement pastes (Figs. 1 and 2) show that porosity values issued from oven-drying at 60°C and vacuum-drying were very similar. Average relative discrepancy is about 1.5% for CEM I pastes and about 4% for CEM V pastes. The freeze-drying method provided slightly underestimated porosity values compared with average porosity values obtained through 60°C oven-drying and vacuum-drying, about 8% for CEM I pastes and 13% for CEM V pastes (in relative). In fact it was observed that, after 7 days, the mass loss was not entirely stable with this method. To reach the same drying efficiency, freeze-drying (sublimation) must be prolonged, especially for dense—low permeable—materials. Water porosity values determined after a 105°C oven-drying were systematically overestimated compared with porosity values obtained after 60°C oven-drying and vacuum-drying. For both types of cement paste, relative overestimation is about 15%.

It is generally considered that, at 105°C, only free water—evaporable water—was removed from porosity. On the other hand, this procedure is usually selected mainly because it is a quicker drying method. In fact, the drying of cementitious phases is a continuous phenomenon and dehydration (nonevaporable water removal) of cement hydrates starts at lower temperatures. We know that gypsum dehydration begins around 80°C [45,46] and that the starting decomposition temperature of ettringite is about 60°C [47]. Drying is responsible for the structural and physical collapse of hydrates like monosulfoaluminate (AFm) and AFt phases [29]. The temperature at which the decomposition of C-S-H initiates is not well established but C-S-H are partially dehydrated at 105°C. Pore structure is thus affected [48]. We will see later on how the pore structure of cement-based materials can be strongly altered by the drying technique.

Experimental total water porosity values, obtained after oven-drying at 60°C and 105°C on various w/c CEM I pastes aged 78 months, were compared with porosity values

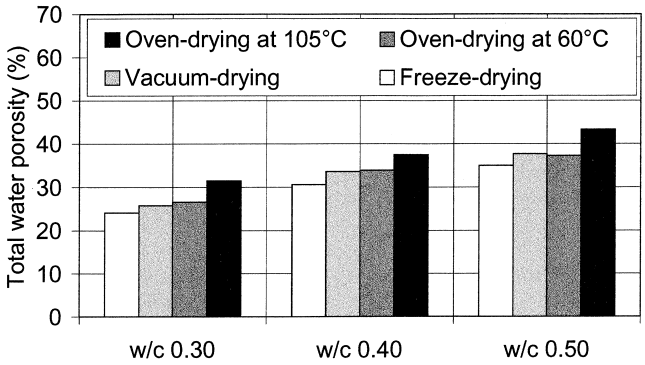

Fig. 1. CEM I total water porosity evolution in function of the drying technique.

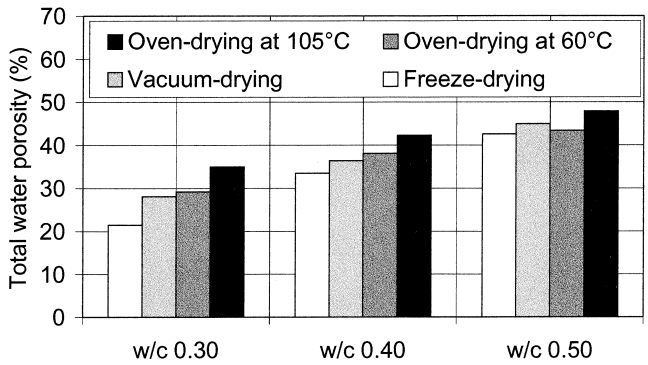

Fig. 2. CEM V total water porosity evolution in function of the drying technique.

estimated through the Powers–Brownyard model [49,50]. Total porosity (ϕ_t), which is equal to the sum of capillary porosity and hydrates porosity (gel pores), was calculated with the following general relation (Eq. (3)):

$$\phi_t = \phi_0 - 0.55m(1-\phi_0) \quad (3)$$

where ϕ_t is the total porosity, ϕ_0 is the initial porosity, and m is the hydration rate. If we consider the hydration of cement-based materials cured under water, then the w/c ratio critical value below which complete hydration cannot occur can be taken equal to 0.38 [51]. Initial porosity was calculated as follows (Eq. (4)):

$$\phi_0 = \frac{w/c}{w/c + 0.313}. \quad (4)$$

Experimental and calculated porosities are compared in Fig. 3. Relative discrepancy between porosity values is about 10%. It should be recalled that, for the Powers–Brownyard approach, the critical w/c is an essential parameter. In literature, this parameter generally varies between 0.36 and 0.38. Moreover, in this model, free water roughly corresponds to the quantity of water removed at 105°C [49]. We previously emphasised that, at this temperature, cement hydrates were already partly dehydrated. Thus, porosity values obtained through 105°C oven-drying are obviously overestimated. This is why it was considered that oven-drying at 60°C allows to estimate total water porosity of cement-based materials in a more realistic way.

Average water porosity obtained through 60°C oven-drying and vacuum-drying and mercury porosity are compared in Fig. 4. It should be emphasised that mercury porosimetry is a qualitative tool. Quantitative pore space characterisation is not complete because the range of pore accesses is limited to approximately 375 μm to around 3 nm (depending on the apparatus). All porosities below and above these limits are not detected. This is why mercury porosimetry gives an underestimated value of total porosity for cement-based materials compared with

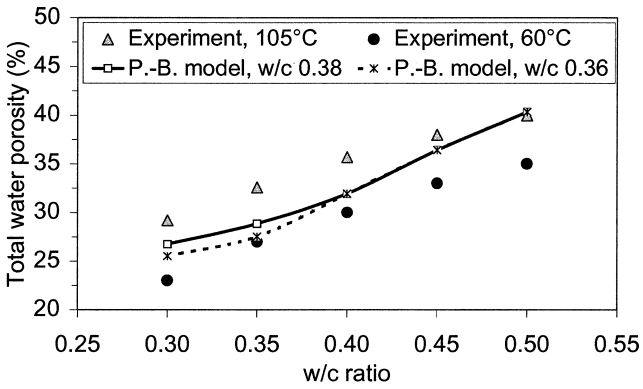

Fig. 3. Correlation between experimental water porosity obtained through 60°C and 105°C oven-drying and porosity estimated through Powers–Brownyard model considering 0.36 and 0.38 critical w/c ratio.

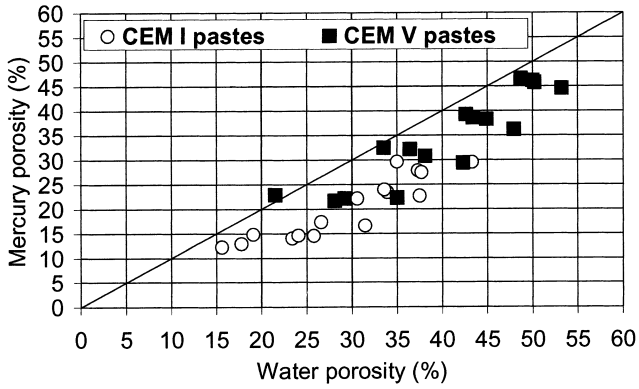

Fig. 4. Relationship between total water and mercury porosity for CEM I and CEM V pastes.

water porosity. As is also well known, water penetration pore access range is much wider and goes down around 0.5 nm [52].

5.2. Pore microstructure

The identification of cement-based materials microstructure (pore size distribution) is essential to understand and to model transport mechanisms such as diffusion and convection. It is thus a priority to know what is the influence of the drying technique on pore structure when performing mercury porosimetry investigation. The effect of the four drying methods on materials MIP spectrum is analysed in the following paragraphs. Cumulative intruded pore volume curves obtained for CEM I and CEM V pastes with the different drying techniques are provided in Fig. 5. Fig. 6 shows the corresponding pore size distributions (differential intruded pore volume).

From Fig. 5, it was observed that the final intruded pore volumes obtained through the different methods can be regarded as very close, but the intrusion curves shape varies quite a lot depending on the technique. It can thus be concluded that total mercury porosity values were not so much influenced by the drying technique (Table 3). The mercury intrusion test only provides part of the porous space image. Moreover, various threshold pore accesses are easily detectable and reflect the pore microstructure as well as the connectivity of porous space. Concerning the threshold pore diameters, it was observed that the values were located in a quite narrow range, between 0.03 and 0.18 μm on average (Table 3). These values comply with those found by Feldman and Beaudoin [21] with 0.45 w/c OPC pastes dried by various techniques. Data obtained on CEM I and CEM V pastes clearly showed that the lowest threshold values were obtained with the freeze-drying. This result may indicate a lower alteration of the pore structure when using this technique.

For CEM I pastes, with pore access of up to about 4 nm, intruded volumes decrease when removed from oven-drying at 105°C, to oven-drying at 60°C, to vacuum-

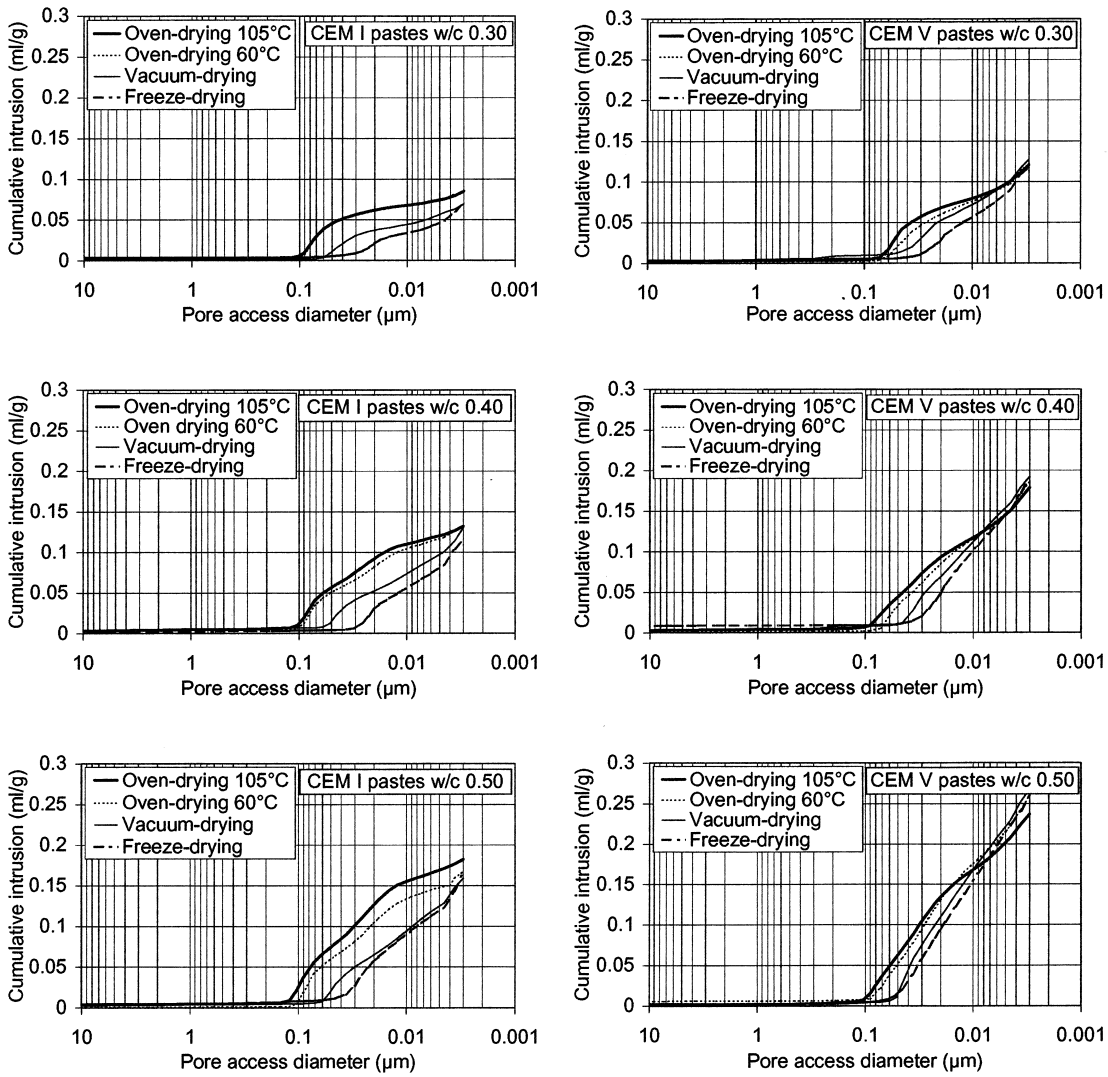

Fig. 5. Drying technique influence on CEM I (left) and CEM V (right) pastes cumulative intruded pore volume, w/c 0.30, 0.40, and 0.50.

drying and to freeze-drying. It is generally within this pore access range—0.04 to 0.03 μm—that the intruded volume obtained through freeze-drying increases and meets the intruded volume obtained through other methods. This phenomenon was also observed for CEM V pastes but with higher pore access range. It could be associated to potential damages generated during the freezing and/or sublimation operation. These results could suggest that damages induced by freeze-drying, in this pore domain (nanoporosity), are probably bigger than with the other techniques.

Differential intrusion curves in Fig. 6 provide extended information on pore structure evolution. For CEM I pastes, pore size distributions are generally characterised by three main classes of pore access. Pore accesses located in the vicinity of 0.1 μm and a little above that limit are usually associated to capillary porosity (macroporosity). A second and a third class of pore access are generally detected in the regions located around 0.02 μm (microporosity) and around a few nanometers (nanoporosity). This pore space domain describes the pore accesses of C-S-H that can be split up into outer and inner C-S-H [53]. The occurrences of such pore accesses depend on the w/c ratio and on the material age and curing conditions.

It was already mentioned that, according to the Powers–Brownyard model, under the 0.38 threshold w/c ratio, all the water is consumed during the hydration process and that, theoretically, no capillary porosity can be detected. On the other hand, recent studies pointed out that macroporosity was not only related to water excess but also to self-desiccation [54]. It should also be emphasised that the position of some porosity peaks does not only depend on the real access size of the pore but also on their connectivity. It was observed that for the peaks associated to macroporosity, the position of the peaks shifts towards smaller access size as connectivity decreases. On the opposite, the peaks related to microporosity and nanoporosity do not evolve if connectivity changes [55].

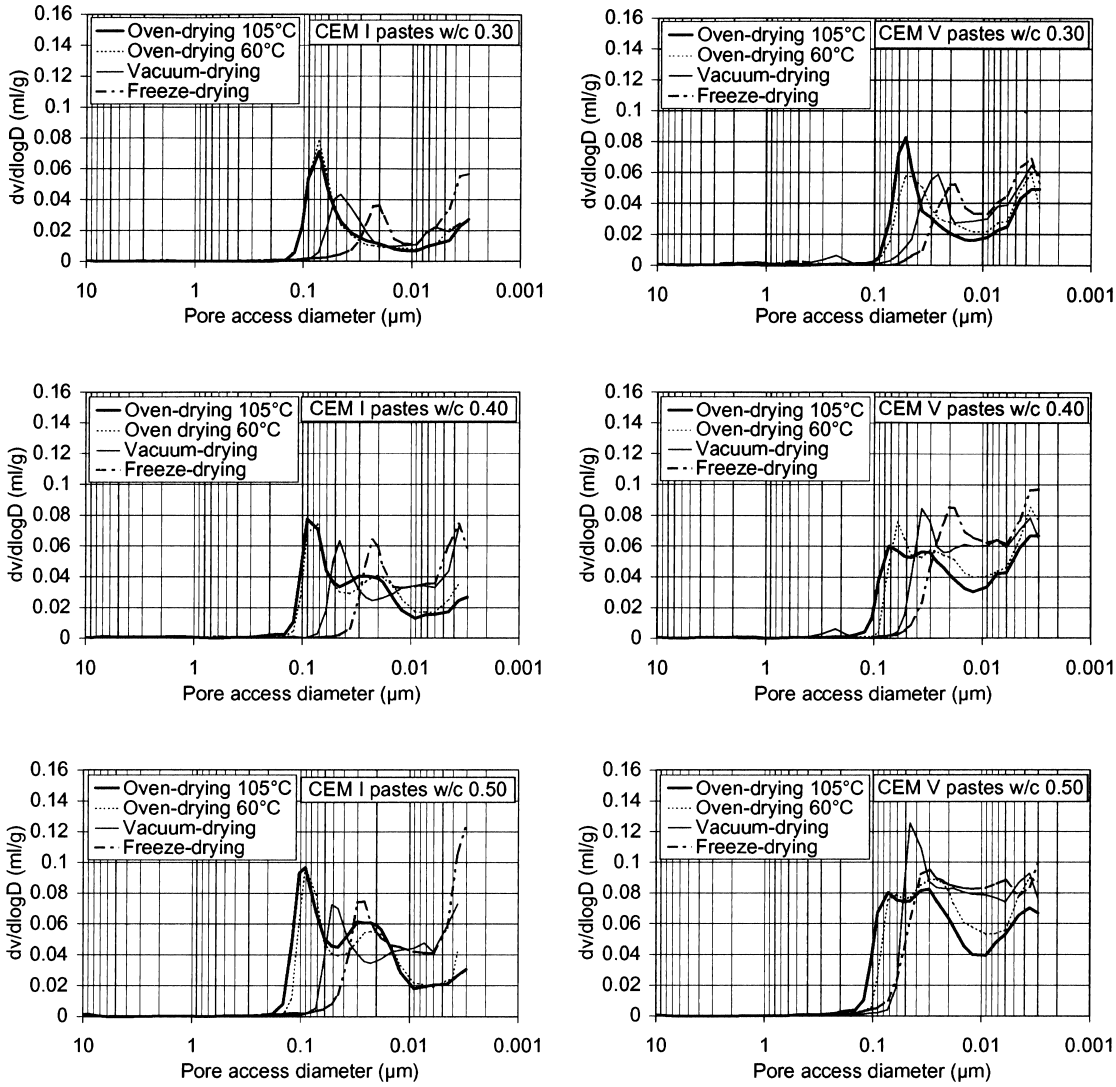

Fig. 6. Drying technique influence on CEM I (left) and CEM V (right) pastes pore size distribution, w/c 0.30, 0.40, and 0.50.

Concerning the effect of drying on CEM I paste microstructure, it was observed that the materials treated at 60°C and 105°C were characterised by similar pore size distributions. These treatments generate a large capillary porosity with pore accesses located around 0.08 μm. For the vacuum-drying technique, a macroporosity is observed for smaller pore accesses around 0.05 μm with a lower peak intensity. The results also show that, for freeze-drying, no capillary pore access is detected. The pore accesses that can be associated to outer C-S-H are localised around 0.02 μm, whatever the drying method. Finally, it was observed that the residual peak related to the nanoporosity (around 0.003 μm) and corresponding to inner C-S-H is larger after vacuum-drying and freeze-drying.

As a conclusion, oven-drying at 60°C and 105°C generates a large porosity that can be associated to the capillary domain (macroporosity). This porosity is less significant with the vacuum-drying technique and is not detected with the freeze-drying method. Previous studies [48,56] already suggested that, during drying at 105°C (and 60°C), capillary effects are associated with hydrostatic stresses generating damages that can alter the pore structure mainly by rearranging the hydration products. In other words, it is considered that the stresses related to surface tension of the receding water menisci generate a collapse of some of the fine pores and consequently an increase of the volume of larger pores [38]. Cement hydrates desiccation is also probably responsible for microcrack generation. During sublimation operation, the solid phase (ice) is converted directly into gas and thus freeze-drying method softens capillary stress effects [30]. This result is quite important, suggesting that the freeze-drying technique is a less damaging method for hardened cement paste pore structure investigation. However, it was observed that freeze-drying provokes a greater alteration of fine pores related to inner and outer C-S-H, above all in the nanoporosity domain (inner C-S-H). This phenomenon could be related to compressive stress (pore retraction) during freezing opera-

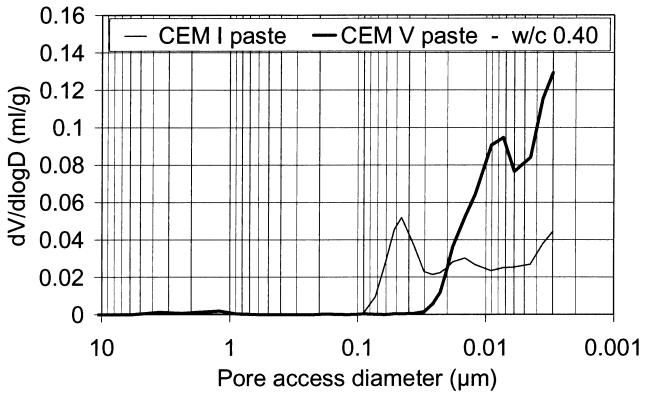

Fig. 7. Comparison of MIP pore size distributions of CEM I paste (aged 28 months) and CEM V paste (aged 36 months), w/c 0.40.

tion and/or to mechanism operating during sublimation. It should also be mentioned that the solvent replacement drying technique proved to be less damaging for fine pore size regions (nanoporosity). However, this method seems to be more time consuming than freeze-drying. Konecny and Naqvi [28] provided arguments that suggested that the freeze-drying technique also preserved, to some extent, the fine pore region. On the other hand, Feldman and Beaudoin [21] carried out an extended comparative study on the pretreatments to be applied to hardened cement pastes for MIP test. The solvent exchange technique, vacuum-drying with or without oven-drying, and predrying at 11% relative humidity were investigated. They recommended the use of the solvent replacement technique using isopropanol as a suitable drying technique for such a material. Unfortunately, the freeze-drying technique was not studied in this work by the authors.

Similar interpretations can be drawn with CEM V cement pastes pore structure. First, it should be recalled that CEM V pastes are characterised by a higher porosity (Table 3) and do not usually show any capillary porosity (Fig. 7). As is also well known, hydration of CEM V materials is only completed after several years while, for CEM I, complete hydration is reached within a few months. Therefore, CEM V pastes should not be regarded as fully hydrated materials.

For CEM V pastes, a similar pore size distribution was observed for oven-dryings at 60°C and 105°C. This type of drying generates a capillary porosity located around 0.05-μm pore access. With the vacuum-drying method, microporosity seems to shift to pore accesses around 0.03 μm, but in that pore access range it is unclear whether we are still in the macroporosity domain or in the microporosity domain (outer C-S-H). On the other hand, there is no capillary porosity on pore size distribution obtained after freeze-drying. Finally, as far as nanoporosity intensity is concerned, the discrepancy between all the drying methods is smaller than for CEM I pastes. Though the effect of the various drying methods was quite similar for both types of cement paste, the phenomena observed for CEM V cement pastes could have been more significant with more mature materials.

For concretes, only three types of drying methods were compared: oven-drying at 60°C and 105°C and freeze-drying. Concrete probes were oven-dried for 2–3 months until stable mass loss was reached. Results obtained for concretes are illustrated in Fig. 8 (cumulative intruded pore volume) and Fig. 9 (differential intruded pore volume). They show that concrete pore structure is deeply altered by oven-drying. Similar pore size distributions were obtained by recent studies for high-performance concrete submitted to 105°C [57,58]. For CEM I concrete, exposure to 60°C and 105°C lead to similar pore size distributions and to the appearance of pore accesses located in the regions between 0.2 and 0.02 μm (Fig. 9). This pore family was not detected for freeze-drying. CEM V concrete pore size distributions showed comparable phenomena with again the development of a large capillary porosity after oven-drying, above all at 105°C (Fig. 9). These results confirm the great impact of oven-drying on concrete pore structure. For concretes, there is an additional effect due to aggregates for which thermal expansion may be very different from the hardened paste one [59]. Data acquired with concretes confirm that freeze-drying is a suitable pretreatment to investigate the pore structure of cement-based materials by MIP. For the concretes study, it can be added that a 1°C/min heating rate does not significantly reduce the pore structure damaging. In order to precisely identify the types of damage

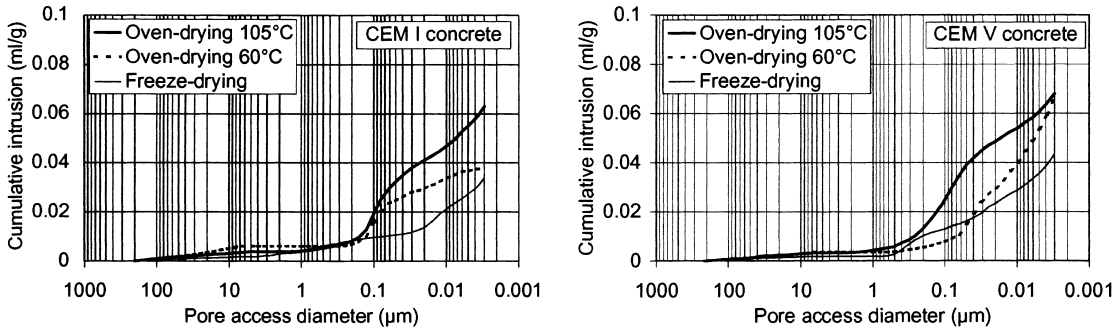

Fig. 8. Drying technique influence on CEM I (left) and CEM V (right) concretes cumulative intruded pore volume (w/c 0.43).

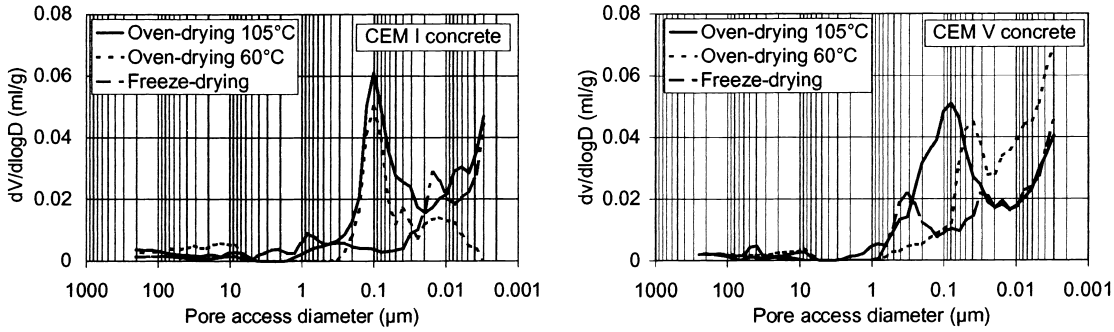

Fig. 9. Drying technique influence on CEM I (left) and CEM V (right) concretes pore size distribution (w/c 0.43).

generated by the various drying techniques, complementary works could be performed using image analysis. This technique could provide useful information on microcracking quantification [60].

6. Conclusion

MIP tests performed after different drying methods on various cement-based materials allowed to recall that much attention should be paid to the choice of such a technique for pore structure investigation. Porosity and pore size distribution are essential parameters to describe materials transport and mechanical properties. Chemical degradation and mechanical models need the most complete—reproducible/meaningful—information on cementitious materials microstructure. Experimental results obtained in this study on CEM I and CEM V pastes and concretes showed that oven-drying at 105°C leads to an overestimation of total porosity. In such a condition, hydrates like ettringite and C-S-H probably lose a significant amount of nonevaporable water. Water porosity obtained through oven-drying at 60°C and vacuum-drying were very close and probably allow to estimate the total porosity more realistically. Total porosity data obtained through freeze-drying proved to be similar. For pore structure, mercury intrusion curves showed that, globally, oven-dryings at 60°C and 105°C are responsible for a large capillary porosity that can be attributed to capillary stress, cement hydrates (ettringite, Afm, C-S-H) desiccation and potential microcrack generation in relationship with internal thermohydric stress. This pore access class, located around 0.1 μm, is therefore associated with a phenomenon that can be considered an artefact related to the drying technique. Similar conclusion was reached for the vacuum-drying technique. Oven-drying at such temperatures is obviously an unsuitable procedure to preserve the fragile microstructure of cement-based materials. Freeze-drying is probably an interesting and adequate alternative drying technique for the MIP investigation of cementitious materials. This method does not introduce artificial porosity in the capillary porosity domain. On the other hand, it was observed that the threshold pore access diameter was significantly lower with this technique compared to those obtained with the other drying procedures. It was, however, observed that this technique probably generates limited but significant damages, related to thermomechanical stress in the region (inner C-S-H porosity). Results obtained on concretes confirmed the impact of oven-drying on pore structure and suggested that freeze-drying is a suitable procedure to be applied to the study of cement-based materials pore structure using MIP. Additional works on solvent replacement technique could be performed to complete this study.

Acknowledgments

Experimental data were partly obtained in the framework of a study supported by the French Agence Nationale pour la gestion des déchets radioactifs (ANDRA) and by Electricité de France (EdF). The author gratefully acknowledges Mr. M. Pin, from CEA, for performing the mercury intrusion porosity tests.

References

[1] F.P. Glasser, M. Atkins, Cements in radioactive waste disposal, MRS Bull. (1994) 33–38 (December).
[2] C.R. Wilding, The performance of cement based systems, Cem. Concr. Res. 22 (2) (1992) 299–310.
[3] F. Adenot, M. Buil, Modelling of corrosion of cement paste by deionized water, Cem. Concr. Res. 22 (3) (1992) 489–495.
[4] F. Adenot, C. Richet, P. Faucon, Long-term prediction of concrete durability in radioactive waste management: Influence of the pH of the aggressive solution, Int. Conf. Eng. Mater., Ottawa 2 (1997) 107.
[5] P. Faucon, F. Adenot, J.F. Jacquinot, J.C. Petit, R. Cabrillac, M. Jorda, Long-term behaviour of cement pastes used for nuclear waste disposal: Review of physico-chemical mechanisms of waste degradation, Cem. Concr. Res. 28 (6) (1998) 847–857.
[6] M. Mainguy, C. Tognazzi, J.M. Torrenti, F. Adenot, Modelling of leaching in pure cement paste and mortar, Cem. Concr. Res. 30 (1) (2000) 83–90.
[7] C. Carde, R. François, J.M. Torrenti, Leaching of both calcium hydroxide and C-S-H from cement paste: Modeling the mechanical behaviour, Cem. Concr. Res. 26 (8) (1996) 1257–1268.
[8] P. Bouniol, P. Thouvenot, Aspect physico-chimique du comportement des bétons sous irradiation, J. Chim. Phys. 94 (1997) 410–417.
[9] F. Badouix, P. Le Bescop, P. Lovera, F. Adenot, J.P. Bournazel, Carbonatation d'une pâte de CPA-CEM I au cours d'un essai de lixivaia-

tion à pH de 8.5 et modélisation d'un cas simplifié de carbonatation, XVI^{éme} Rencontres Univ. Génie Civil OE'98, Reims, France I (1998) 49–56.
[10] G. Li, P. Le Bescop, M. Moranville, The U phase formation in cement-based systems containing high amounts of Na_2SO_4, Cem. Concr. Res. 26 (1) (1996) 27–33.
[11] P. Lovera, P. Le Bescop, F. Adenot, G. Li, Y. Tanaka, E. Owaki, Physico-chemical transformations of sulphated compounds during the leaching of highly sulphated cemented wastes, Cem. Concr. Res. 27 (10) (1997) 1523–1532.
[12] P. Lovera, C. Gallé, P. Le Bescop, Towards an intrinsic relationship between diffusion coefficients and microscopic features of cements, MRS Conf., Sydney, Australia, 27–31 August, 2000.
[13] C. Gallé, J.F. Daian, Gas permeability of unsaturated cement based materials: Application of a multiscale network model, Mag. Concr. Res. 52 (4) (2000) 251–263.
[14] D.N. Winslow, S. Diamond, A mercury porosimetry study of the evolution of porosity in Portland cement, J. Mater. 5 (3) (1970) 564–585.
[15] R.F. Feldman, J.J. Beaudoin, Microstructure and strength of hydrated cement, Cem. Concr. Res. 6 (3) (1976) 398–400.
[16] J.J. Beaudoin, Porosity measurement of some hydrated cementitious systems by high pressure mercury intrusion—microstructural limitations, Cem. Concr. Res. 9 (6) (1979) 771–781.
[17] F.S. Rostasy, R. Weiß, G. Wiedemann, Changes on pore structure of cement mortars due to temperature, Cem. Concr. Res. 10 (2) (1980) 157–164.
[18] R.F. Feldman, Pore structure damage in blended cements caused by mercury intrusion, J. Am. Ceram. Soc. 67 (1) (1984) 30–33.
[19] B.K. Nyame, Permeability of normal and lightweight mortars, Mag. Concr. Res. 37 (130) (1985) 44–48.
[20] D.C. Okpala, Pore structure of hardened cement paste and mortar, Int. JCCLC 11 (4) (1989) 245–254.
[21] R.F. Feldman, J.J. Beaudoin, Pretreatment of hardened hydrated cement pastes for mercury intrusion measurements, Cem. Concr. Res. 21 (2/3) (1991) 297–308.
[22] J.H.D. Hampton, M.D.A. Thomas, Modelling relationships between permeability and cement paste pore microstructures, Cem. Concr. Res. 23 (6) (1993) 1317–1330.
[23] A.S. El-Dieb, R.D. Hooton, Evaluation of Katz–Thompson model for estimating the water permeability of cement-based materials from mercury intrusion porosimetry data, Cem. Concr. Res. 24 (3) (1994) 443–455.
[24] J. Marchand, H. Homain, S. Diamond, M. Pigeon, H. Guiraud, The microstructure of dry concrete products, Cem. Concr. Res. 26 (3) (1996) 427–438.
[25] M.A.I. Laskar, R. Kumar, B. Bhattacharjee, Some aspects of the evaluation of concrete through mercury intrusion porosimetry, Cem. Concr. Res. 27 (1) (1997) 93–105.
[26] R.A. Cook, K.C. Hover, Mercury porosimetry of hardened cement pastes, Cem. Concr. Res. 29 (6) (1999) 933–943.
[27] S. Diamond, Mercury porosimetry, an inappropriate method for the measurement of pore size distributions in cement-based materials, Cem. Concr. Res. 30 (10) (2000) 1517–1525.
[28] L. Konecny, S.J. Naqvi, The effect of different drying techniques on the pore size distribution of blended cement mortars, Cem. Concr. Res. 23 (5) (1993) 1223–1228.
[29] L. Zhang, F.P. Glasser, Critical examination of drying damage to cement pastes, Adv. Cem. Res. 12 (2) (2000) 79–88.
[30] P. Delage, F.M. Pellerin, Influence de la lyophilisation sur la structure d'une argile sensible du Québec, Clay Miner. 19 (1984) 151–160.
[31] D.H. Bager, E.J. Sellevold, Ice formation in hardened cement paste: Part III. Slow resaturation of room temperature cured pastes, Cem. Concr. Res. 17 (1) (1987) 1–11.
[32] A. Kumar, D.M. Roy, The effect of desiccation on the porosity and pore structure of freeze-dried hardened Portland cement and slag-blended pastes, Cem. Concr. Res. 16 (1) (1986) 74–78.
[33] L.J. Parrott, Effect of drying history upon the exchange of pore water with methanol and upon subsequent methanol sorption behaviour in hydrated alite paste, Cem. Concr. Res. 11 (5) (1981) 651–658.
[34] L.J. Parrott, Thermogravimetric and sorption studies of methanol exchange in alite paste, Cem. Concr. Res. 13 (1) (1983) 18–22.
[35] L.J. Parrott, An examination of two methods for studying diffusion kinetics in hydrated cements, Mater. Struct. 17 (98) (1984) 131–137.
[36] R.F. Feldman, Diffusion measurements in cement paste by water replacement using propan-2-ol, Cem. Concr. Res. 17 (4) (1987) 602–612.
[37] R.L. Day, B.K. Marsh, Measurement of porosity in blended cement pastes, Cem. Concr. Res. 18 (1) (1988) 63–73.
[38] M.D.A. Thomas, The suitability of solvent exchange techniques for studying the pore structure of hardened cement paste, Adv. Cem. Res. 2 (5) (1989) 29–34.
[39] N. Hearn, R.D. Hooton, Sample mass and dimension effects on mercury intrusion porosimetry results, Cem. Concr. Res. 22 (5) (1992) 970–980.
[40] R.L. Day, Reactions between methanol and Portland cement paste, Cem. Concr. Res. 11 (3) (1981) 341–349.
[41] H.F.W. Taylor, A.B. Turner, Reactions of tricalcium silicate paste with organic liquids, Cem. Concr. Res. 17 (4) (1987) 613–623.
[42] D.C. Hughes, N.L. Crossley, Pore structure characterisation of GGB/OPC grouts using solvent techniques, Cem. Concr. Res. 24 (7) (1994) 1255–1266.
[43] J.J. Beaudoin, P. Gu, J. Marchand, B. Tamtsia, R.E. Myers, Z. Liu, Solvent replacement studies of hydrated Portland cement systems: The role of calcium hydroxide, Adv. Cem. Based Mater. 8 (2) (1998) 56–65.
[44] H.C. Gran, E.W. Hansen, Exchange rates of ethanol with water in water-saturated cement pastes probed by NMR, Adv. Cem. Based Mater. 8 (3/4) (1998) 108–117.
[45] D.N. Winslow, D. Liu, The pore structure of paste in concrete, Cem. Concr. Res. 20 (5) (1990) 227–235.
[46] V. Baroghel-Bouny, Caractérisation des Pàtes de Ciment et des Bétons, Méthodes, Analyse, Interprétations, LCPC Publications, Paris, 1994.
[47] M. Murat, Stabilité thermique des aluminates de calcium hydratés et phases apparentées. Caractérisation par les méthodes thermoanalytiques, Aluminates Calcium, Int. Semin., Turin, Italy, (1982) 59–84.
[48] M. Moukwa, P.C. Aïtcin, The effect of drying on cement pastes pore structure as determined by mercury porosimetry, Cem. Concr. Res. 18 (5) (1988) 745–752.
[49] T.C. Powers, T.L. Brownyard, Studies of the physical properties of hardened Portland cement paste, J. Am. Concr. Inst. 22 (9) (1947) 971–992.
[50] A.M. Neville, Durability of Concrete, Properties of Concrete, Longman, London, UK, 1981.
[51] T.C. Powers, The physical structure and engineering properties of concrete. J. PCA Res. Dev. Lab. 90 (1958) 1–28.
[52] K. Xu, Structures multiechelles, Modèles pour la description des matériaux poreux et l'estimation de leurs propriétés de transport, Thèse, Université Joseph Fourrier, Grenoble, 1995.
[53] D.P. Bentz, K.A. Snyder, P.E. Stutzman, Hydration of Portland cement: The effect of curing conditions, in: H. Justnes (Ed.), Proc. 10th Int. Congr. Chem. Cem., Gothenburg, Sweden 2 (1997), 2iio78.
[54] H.F.W. Taylor, Cement Chemistry, second ed., Thomas Telford Publishing, London, 1997.
[55] R. Vocka, C. Gallé, M. Dubois, P. Lovera, Mercury intrusion porosimetry and hierarchical structure of cement pastes: Theory and experiment, Cem. Concr. Res. 30 (4) (2000) 521–527.
[56] T.C. Powers, T.L. Brownyard, Studies of the physical properties of hardened Portland cement paste, J. Am. Concr. Inst. 18 (5) (1947) 549–602.
[57] M. Tsimbrovska, P. Kalifa, D. Quenard, J.F. Daian, High performance concretes at elevated temperature: Permeability and micro-

structure, Trans. 14th Int. Conf. Struct. Mech. Reactor Technol. HW/6 (SmiRT 14), Lyon, France, (1997) 475–482.
[58] Y.N. Chan, X. Luo, W. Sun, Compressive strength and pore structure of high-performance concrete after exposure to high temperature up to 800°C, Cem. Concr. Res. 30 (2) (2000) 247–251.
[59] C. Gallé, J. Sercombe, M. Pin, G. Arcier, P. Bouniol, Behaviour of high performance concrete under high temperature (60–450°C) for surface long-term storage: Thermo-hydro-mechanical residual properties, MRS Conf., Sydney, Australia, 27–31 August, 2000.
[60] A. Ammouche, D. Breysse, H. Homain, O. Didry, J. Marchand, A new image analysis technique for quantitative assessment of microcracks in cement based materials, Cem. Concr. Res. 30 (1) (2000) 25–35.